JACS
JOURNAL OF THE AMERICAN CHEMICAL SOCIETY
Cite This: J. Am. Chem. Soc. XXXX, XXX, XXX−XXX
Communication
pubs.acs.org/JACS

# Selective Vapor Pressure Dependent Proton Transport in a Metal−Organic Framework with Two Distinct Hydrophilic Pores

Sarah S. Park, Adam J. Rieth, Christopher H. Hendon, and Mircea Dincă*

Department of Chemistry, Massachusetts Institute of Technology, 77 Massachusetts Avenue, Cambridge, Massachusetts 02139, United States

Supporting Information

**ABSTRACT:** The mechanism of proton conductivity in porous solids (i.e., Grotthuss or vehicular) is related to the structure and chemical environment of the pores. Direct observation of structure−function relationships is difficult because state-of-the-art solid proton conductors are often amorphous. Here, we present a systematic elucidation of two distinct proton transport pathways within **MIT-25**, a mesoporous metal−organic framework that exhibits parallel channels of ∼27 Å and ∼4.5 Å width. We characterize transport through these pores using temperature- and humidity-dependent proton conductivity measurements and density functional theory. Through control of vapor pressure we are able to sequentially fill the small and large pores, promoting proton conductivity with distinct activation energies at low and high relative humidity, respectively.

One of the limiting factors in the design and implementation of highly efficient fuel cells is the chemical performance and stability of the electrolyte.[1−3] Among solid state electrolytes for intermediate- and high-temperature fuel cells, metal-organic frameworks (MOFs) provide compelling attributes including tunable hydrophilicity and pore size.[4−8] From a design perspective, MOFs are attractive also because they provide crystallographically defined proton conduction pathways,[9−11] in contrast to polymeric electrolytes such as Nafion, a highly conductive but amorphous material.[12] Because electrolyte performance is intimately related to both pore size and the polarity of the proton-conducting channels, detailed characterization of the proton conduction pathways can provide important clues for the design of better electrolytes.[4−7] It is this broad compositional and structural tunability that has led to important advances in the use of MOFs as solid electrolytes for fuel cells.[13−19]

Assigning a specific mechanism to proton conduction in confined pores is difficult, however, because the mechanisms are typically convoluted and the activation energies measured are often averages for overall transport. Indeed, although the Grotthuss (i.e., hopping)[20] and the vehicular (i.e., diffusive)[21] mechanisms are typically distinguished by the difference in their specific activation energies ($E_a$), with the former exhibiting a lower barrier for transport, only rarely can they be distinguished under normal operating conditions.[22−27]

The Grotthuss mechanism is thought to occur through the dissociation of an H-bonded proton, and subsequent relay through the material.[20] The $E_a$ for this process is usually smaller than ∼0.4 eV, the typical O···H hydrogen bond dissociation energy. In contrast, the vehicular mechanism features larger $E_a$ associated with a combination of solvent rearrangement and ion diffusion through a dielectric medium. The activation energy is intimately related to both the topology of the conductive medium and the concentration of charge carriers/hopping sites. Specifically, the $E_a$ will decrease with increasing relative humidity (RH) regardless of transport mechanism. If the Grotthuss mechanism is operative, increasing RH decreases $E_a$ owing to the increase in the number of available hopping sites (i.e., water molecules) in a given volume.[28] If proton transport is vehicular, $E_a$ decreases with RH because diffusion of the proton carrying unit (i.e., hydronium ions) is more facile in a pore filled with water than in an empty pore. Here, we report that **MIT-25**, a mesoporous MOF with two distinct channels, is capable of proton conduction that depends on the degree of pore filling. This study provides valuable insight into the operative design principles for next generation solid-state MOF electrolytes.

$Mg_2H_6(H_3O)(TTFTB)_3$ (**MIT-25**, $TTFTB^{4-}$ = tetrathiafulvalene-tetrabenzoate)[29] is mesoporous and thus unlikely to exhibit high absolute proton conductivity or utility as a proton conducting dense membrane. Regardless, its unprecedented large proton content (8 acidic protons per formula unit) and compositionally integral hydronium ions make it an excellent platform for fundamental investigations of proton transport (Figure S1). As shown in Figure 1a, **MIT-25** exhibits two cylindrical parallel pores: the larger 27 Å-wide mesopore is decorated with two structurally integral $\mu_2$-H-bridged carboxylic acids per $Mg^{2+}$ center. The small 4.5 Å-wide pore contains an additional pair of $\mu_2$-H-bridged carboxylates that protrude into the pore and give rise to a helical channel (Figure 1b and c). Although the stoichiometric $H_3O^+$ ion resides primarily in the small pore and occupies part of the void volume, there remains ample room within this small pore for additional guest $H_2O$ molecules. We thus surmised that the small pore could afford an ideal environment for Grotthuss-type proton conductivity with no contribution from the mesopores, which otherwise could remain empty to provide a highly porous, proton-conducting MOF.

The adsorption isotherm for water vapor in desolvated **MIT-25**, shown in Figure 2, is indeed characteristic of water uptake in a material with two distinct pores. The first water uptake step

Received: December 3, 2017
Published: February 2, 2018




DOI: 10.1021/jacs.7b12784
J. Am. Chem. Soc. XXXX, XXX, XXX−XXX

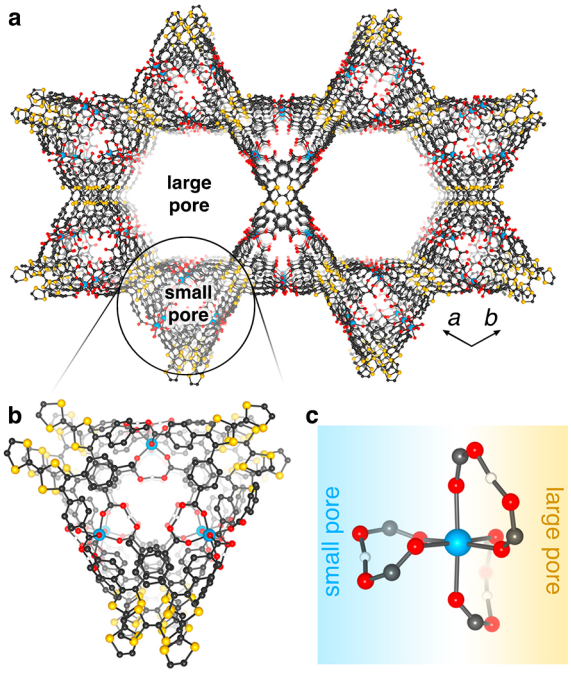


**Figure 1.** (a) Crystal structure of $Mg_2H_6(H_3O)(TTFTB)_3$ (**MIT-25**) viewed along the *c* axis. (b) The small pore contains protruding H-bonded protons. (c) The local coordination environment of each $Mg^{2+}$ center: one $\mu_2$-H-bridged carboxylic acid points into the small pore, and two $\mu_2$-H-bridged carboxylic acids run along the walls of the large pore.

at extremely low RH is associated with adsorption in a very hydrophilic pore, likely the small pore. This confirms that despite partial occupation by $H_3O^+$, water is still absorbed and intercalated through this narrow channel. A second adsorption step, at approximately 50% RH, is associated with a slightly less hydrophilic pore and is in line with what would be expected for the larger, more hydrophobic pore. At even higher pressures (i.e., RH), the isotherm indicates a persistent uptake of water, characteristic of structural swelling. This swelling could be attributed for instance to further oxidation of TTF causing a flattening of the TTF core, an effect observed recently in other

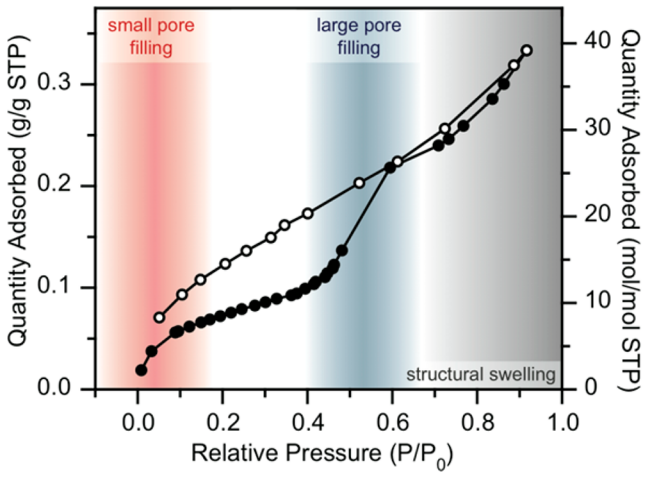


**Figure 2.** Water adsorption (filled circles) and desorption (hollow circles) isotherms in **MIT-25**, indicating filling of the small pore and large pore near 0% and 50% RH, respectively.

TTF-containing MOFs.[30] Although upon desorption **MIT-25** exhibits both retention of water (even at low RH) and loss of long-range crystallinity (Figure S4), chemical connectivity is likely not lost during this step: crystallinity can be recovered by exposing the material to a single drop of the solvent mixture used for its synthesis (*N*,*N*-dimethylformamide/ethanol/water = 3.4:3.8:3). Additionally, even though the crystallinity of **MIT-25** decays above 70% RH, the pore size distribution is conserved (Figure S5), supporting the assertion that short-range order and porosity are maintained and the loss in crystallinity is due to decay in long-range order.

Water filling of the small pore at low RH is also supported by computational studies of the electrostatic potential and pore volume of this channel. (Direct DFT computation of this residual void space is not tractable because (i) the TTFTB organic secondary building unit hosts a delocalized hole, making calculations of hydronium-loaded MIT-25 extremely computationally demanding even with state-of-the-art computational facilities, and (ii) the shallow potential energy surface of the hydronium ion results in extremely slow geometric convergence. There are opportunities for molecular dynamics simulations to provide further insights if a force field can be developed to sufficiently describe the redox behavior of the TTFTB.) It was shown previously that the small pore in hydronium-free **MIT-25** exhibits high and negative potential. This formed the basis for assigning the position of the compositionally integral $H_3O^+$ ion inside this small pore. To determine the possibility of water filling the remaining volume of this pore after occupation by $H_3O^+$, we estimated the total pore volume by analysis of the electrostatic potential as computed for hydronium-free **MIT-25** (Figure 3a, b). Although the small pore features cavities that are much larger than the smallest electrostatic pore opening of 4.42 Å (depicted in Figure 3b), a conservative estimation of the volume of the electrostatic vacuum is given by approximating the pore as a

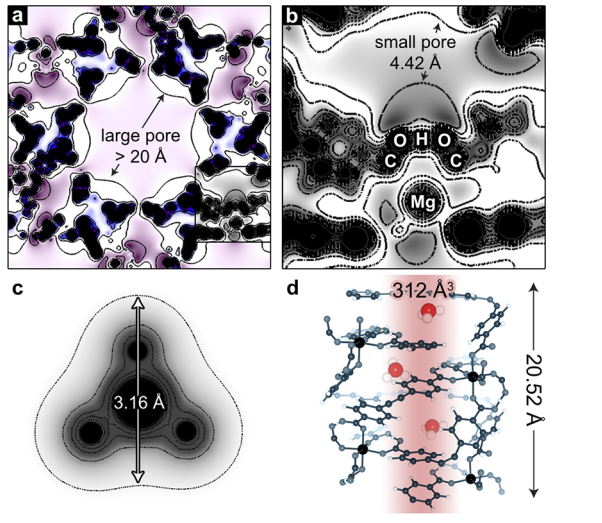


**Figure 3.** (a) Electrostatic potential in **MIT-25** plotted from 5 V (black) to −5 V(purple); grid lines drawn at 1 V intervals. (b) The small pore has an aperture (measured from nuclei centers) of ∼7 Å and an electrostatic potential void of 4.42 Å. (c) This is sufficient to accommodate both hydronium and water. The former has a maximum potential radius of 3.16 Å (given the nature of the cation, the potential is plotted from −100 to 0 V with grid lines drawn at 10 V intervals). (d) Structurally integral hydronium ions within the small pore leave ample room for guest water.


DOI: 10.1021/jacs.7b12784
J. Am. Chem. Soc. XXXX, XXX, XXX−XXX

cylinder with a radius of 2.2 Å. Given a unit cell with a $c$ parameter of 10.26 Å, the estimated electrostatic volume of the small pore is ~156 Å$^3$. Approximating $H_3O^+$ as a sphere with a radius of 1.6 Å and using the analytical electrostatic potential shown in Figure 3c, the electrostatic volume of $H_3O^+$ is ~17 Å$^3$. There are 1.5 $H_3O^+$ ions in a single small pore cylinder, and considering that $H_2O$ has nearly the same electrostatic volume as $H_3O^+$, this calculation suggests that ~7.5 $H_2O$ molecules can be accommodated within the volume of the small pore even in the presence of $H_3O^+$ (Figure 3d). This corresponds to approximately 5 $mmol_{H_2O}/mol_{MOF}$ and is in excellent agreement with the experimentally observed sharp water uptake in **MIT-25** at low RH (Figure 2), as well as thermogravimetric analysis (Figure S6) which suggests that the weight loss from a sample kept at 40% RH (where only the small pore is filled) corresponds to a loss of six $H_2O$ molecules.

To test the potential for proton transport and investigate the nature of the transport mechanism in **MIT-25**, pelletized powder samples were subjected to humidity- and temperature-dependent conductivity measurements using electrochemical impedance spectroscopy (EIS). (Pelletized samples can feature intergrain condensation that likely enhance the maximal proton conductivity observed at high RH.) At constant temperature, the conductivity ($\sigma$) increased with increasing humidity, as expected when protons are involved in conduction (Figure 4a). At 40% RH, the proton conductivity increases from $1.58 \times 10^{-5}$ S/cm at 25 °C to $1.03 \times 10^{-4}$ S/cm at 75 °C, giving an $E_a$ of 0.36 (±0.0074) eV. At 95% RH, the proton conductivity increases from $6.8 \times 10^{-5}$ S/cm at 25 °C to $5.1 \times 10^{-4}$ S/cm at 75 °C, giving an $E_a$ of 0.40 (±0.0009) eV. Despite the relative difference between the $E_a$ values at 40% and 95% RH, the excellent linear fits suggest a possible change in conduction mechanism or transport pathway in shifting from low to high RH.

Based on the water adsorption isotherm, computational analysis, and examination of the pore topology, only the small pore should be filled at less than or equal to 40% RH. Hence, at 40% RH we propose that proton transport occurs exclusively through the small pore, with an activation energy of 0.36 eV that is typically characteristic of the Grotthuss mechanism. The larger pore, which is sufficiently wide to support both Grotthuss and vehicular proton transport, is filled at higher RH, and only above 40% RH. Although the convolution of transport through both small and large pores prevents us from determining the absolute $E_a$ for the large pore, we attribute the unusual observation of increasing $E_a$ with increasing RH to the fact that two distinct pores are competent for proton transport in **MIT-25**, with the contribution from the smaller pore becoming increasingly insignificant for overall transport as water fills the larger pore. The observation of distinct proton transport profiles that correlate closely with the degree of pore filling highlights the unique ability to selectively conduct protons through crystallographic pores using only changes in vapor pressure, a property unique to metal−organic frameworks.

In summary, **MIT-25**, a material that exhibits both micropores and mesopores, allows for controlled step-like filling of each type of pore upon changes in relative humidity, which altogether contribute to distinct proton conduction profiles for the two pores. The humidity-dependent proton conductivity in **MIT-25** highlights the importance of pore aperture in determining the mode of proton conductivity and provides an avenue for future materials design.

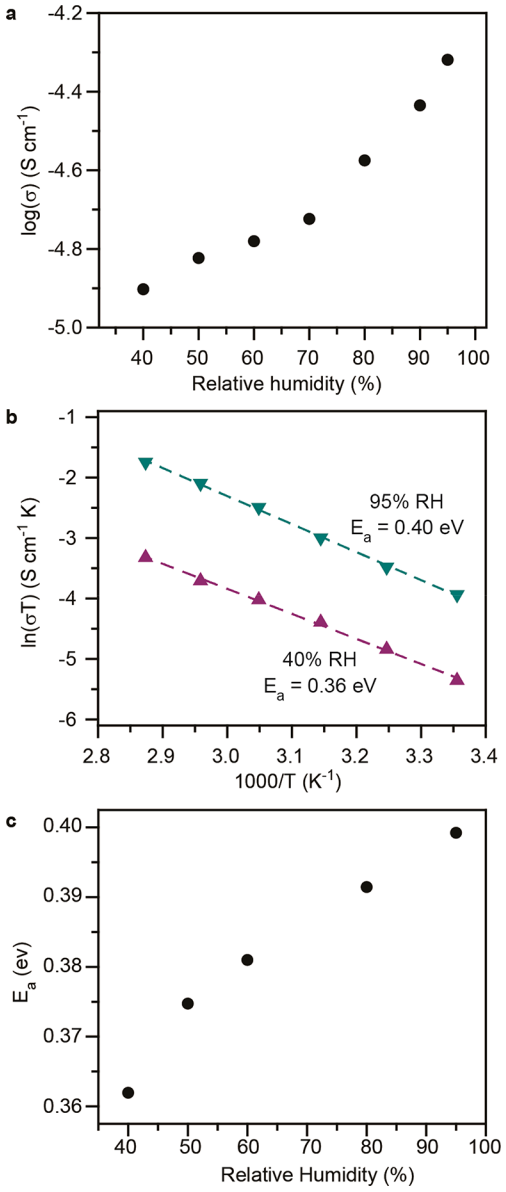


**Figure 4.** (a) Proton conductivity, $\sigma$, as a function of RH at 25 °C. (b) Conductivity at 40% RH (▲) and 95% RH (▼) as a function of temperature in the range 25−75 °C. (c) Activation energy as a function of RH.

## ■ ASSOCIATED CONTENT

### Supporting Information

The Supporting Information is available free of charge on the ACS Publications website at DOI: 10.1021/jacs.7b12784.

Experimental and computational details, PXRD patterns, TGA, and Nyquist plots (PDF)

## ■ AUTHOR INFORMATION

### Corresponding Author

*mdinca@mit.edu

### ORCID

Mircea Dincă: 0000-0002-1262-1264

### Notes

The authors declare no competing financial interest.



DOI: 10.1021/jacs.7b12784
J. Am. Chem. Soc. XXXX, XXX, XXX−XXX

## ■ ACKNOWLEDGMENTS

All experimental work was supported by the U.S. Department of Energy, Office of Science, Office of Basic Energy Sciences (DE-SC0018235). This work used the Extreme Science and Engineering Discovery Environment (XSEDE), which is supported by the NSF (ACI-1053575). S.S.P. was partially supported by an NSF GRFP (1122374). We thank Dr. L. C. H. Moh for helpful discussions on EIS measurements.

## ■ REFERENCES

(1) Dalrymple, S. A.; Shimizu, G. K. H. *J. Am. Chem. Soc.* **2007**, *129*, 12114−12116.
(2) Taylor, J. M.; Vaidhyanathan, R.; Iremonger, S. S.; Shimizu, G. K. H. *J. Am. Chem. Soc.* **2012**, *134*, 14338−14340.
(3) Ramaswamy, P.; Wong, N. E.; Gelfand, B. S.; Shimizu, G. K. H. *J. Am. Chem. Soc.* **2015**, *137*, 7640−7643.
(4) Bureekaew, S.; Horike, S.; Higuchi, M.; Mizuno, M.; Kawamura, T.; Tanaka, D.; Yanai, N.; Kitagawa, S. *Nat. Mater.* **2009**, *8*, 831−836.
(5) Shigematsu, A.; Yamada, T.; Kitagawa, H. *J. Am. Chem. Soc.* **2011**, *133*, 2034−2036.
(6) Kim, S.; Dawson, K. W.; Gelfand, B. S.; Taylor, J. M.; Shimizu, G. K. H. *J. Am. Chem. Soc.* **2013**, *135*, 963−966.
(7) Phang, W. J.; Jo, H.; Lee, W. R.; Song, J. H.; Yoo, K.; Kim, B.; Hong, C. S. *Angew. Chem., Int. Ed.* **2015**, *54*, 5142−5146.
(8) Taylor, J. M.; Dekura, S.; Ikeda, R.; Kitagawa, H. *Chem. Mater.* **2015**, *27*, 2286−2289.
(9) Sahoo, S. C.; Kundu, T.; Banerjee, R. *J. Am. Chem. Soc.* **2011**, *133*, 17950−17958.
(10) Sadakiyo, M.; Yamada, T.; Honda, K.; Matsui, H.; Kitagawa, H. *J. Am. Chem. Soc.* **2014**, *136*, 7701−7707.
(11) Zhang, F.-M.; Dong, L.-Z.; Qin, J.-S.; Guan, W.; Liu, J.; Li, S.-L.; Lu, M.; Lan, Y.-Q.; Su, Z.-M.; Zhou, H.-C. *J. Am. Chem. Soc.* **2017**, *139*, 6183−6189.
(12) Mauritz, K. A.; Moore, R. B. *Chem. Rev.* **2004**, *104*, 4535−4585.
(13) Horike, S.; Umeyama, D.; Kitagawa, S. *Acc. Chem. Res.* **2013**, *46*, 2376−2384.
(14) Yoon, M.; Suh, K.; Natarajan, S.; Kim, K. *Angew. Chem., Int. Ed.* **2013**, *52*, 2688−2700.
(15) Yamada, T.; Otsubo, K.; Makiura, R.; Kitagawa, H. *Chem. Soc. Rev.* **2013**, *42*, 6655−6669.
(16) Ramaswamy, P.; Wong, N. E.; Shimizu, G. K. H. *Chem. Soc. Rev.* **2014**, *43*, 5913−5932.
(17) Nguyen, N. T. T.; Furukawa, H.; Gándara, F.; Trickett, C. A.; Jeong, H. M.; Cordova, K. E.; Yaghi, O. M. *J. Am. Chem. Soc.* **2015**, *137*, 15394−15397.
(18) Peng, Y.; Xu, G.; Hu, Z.; Cheng, Y.; Chi, C.; Yuan, D.; Cheng, H.; Zhao, D. *ACS Appl. Mater. Interfaces* **2016**, *8*, 18505−18512.
(19) Xu, H.; Tao, S.; Jiang, D. *Nat. Mater.* **2016**, *15*, 722−726.
(20) Agmon, N. *Chem. Phys. Lett.* **1995**, *244*, 456−462.
(21) Kreuer, K.-D.; Rabenau, A.; Weppner, W. *Angew. Chem., Int. Ed. Engl.* **1982**, *21*, 208−209.
(22) Liang, X.; Zhang, F.; Feng, W.; Zou, X.; Zhao, C.; Na, H.; Liu, C.; Sun, F.; Zhu, G. *Chem. Sci.* **2013**, *4*, 983−992.
(23) Kawano, R.; Horike, N.; Hijikata, Y.; Kondo, M.; Carné-Sánchez, A.; Larpent, P.; Ikemura, S.; Osaki, T.; Kamiya, K.; Kitagawa, S.; Takeuchi, S.; Furukawa, S. *Chem.* **2017**, *2*, 393−403.
(24) Pili, S.; Argent, S. P.; Morris, C. G.; Rought, P.; García-Sakai, V.; Silverwood, I. P.; Easun, T. L.; Li, M.; Warren, M. R.; Murray, C. A.; Tang, C. C.; Yang, S.; Schröder, M. *J. Am. Chem. Soc.* **2016**, *138*, 6352−6355.
(25) Borges, D. D.; Devautour-Vinot, S.; Jobic, H.; Ollivier, J.; Nouar, F.; Semino, R.; Devic, T.; Serre, C.; Paesani, F.; Maurin, G. *Angew. Chem., Int. Ed.* **2016**, *55*, 3919−3924.
(26) Ye, Y.; Guo, W.; Wang, L.; Li, Z.; Song, Z.; Chen, J.; Zhang, Z.; Xiang, S.; Chen, B. *J. Am. Chem. Soc.* **2017**, *139*, 15604−15607.
(27) Borges, D. D.; Semino, R.; Devautour-Vinot, S.; Jobic, H.; Paesani, F.; Maurin, G. *Chem. Mater.* **2017**, *29*, 1569−1576.
(28) Taylor, J. M.; Dawson, K. W.; Shimizu, G. K. H. *J. Am. Chem. Soc.* **2013**, *135*, 1193−1196.
(29) Park, S. S.; Hendon, C. H.; Fielding, A. J.; Walsh, A.; O'Keeffe, M.; Dincă, M. *J. Am. Chem. Soc.* **2017**, *139*, 3619−3622.
(30) Su, J.; Yuan, S.; Wang, H.-Y.; Huang, L.; Ge, J.-Y.; Joseph, E.; Qin, J.; Cagin, T.; Zuo, J.-L.; Zhou, H.-C. *Nat. Commun.* **2017**, *8*, 2008.


DOI: 10.1021/jacs.7b12784
*J. Am. Chem. Soc.* XXXX, XXX, XXX−XXX